

Ankle and Foot



Giulia Negro, Paolo Simoni, and Hilary Umans

Introduction

Radiological evaluation of the ankle and foot provides essential information for diagnosing congenital and developmental anomalies and guiding orthopaedic treatment.

Alignment of the ankle, hindfoot, midfoot and forefoot is best assessed separately, although they are closely related anatomically and functionally.

A knowledge of the nomenclature is essential for consistent description of foot deformities.

The ankle joint consists of the distal tibia, distal fibula and talus. Inclination of the tibial plafond as seen in the coronal

G. Negro (✉)

Pediatric Imaging Department, Reine Fabiola Children's University Hospital, Université Libre de Bruxelles, Bruxelles, Belgium

P. Simoni

Pediatric Imaging Department, Reine Fabiola Children's University Hospital, Université Libre de Bruxelles, Brussels, Belgium

H. Umans

Albert Einstein College of Medicine Bronx, New York, NY, USA

Lenox Hill Radiology Associates, PC, NYC, USA

© The Author(s), under exclusive license to Springer Nature Switzerland AG 2023

P. Simoni, M. P. Aparisi Gómez (eds.), *Essential Measurements in Pediatric Musculoskeletal Imaging*,

https://doi.org/10.1007/978-3-031-17735-4_10

plane indicates either valgus or varus deformity of the ankle joint. Sagittal plane deformities can be characterised either by dorsiflexion or plantar flexion, which is referred to as “calcaneus” and “equinus”; respectively.

The hindfoot unit consists of the talus and calcaneus; the midfoot consists of the navicular, cuboid and cuneiforms; the forefoot consists of the metatarsals and phalanges.

Hindfoot deformities are described as varus and valgus; midfoot deformities as cavus and planus; and forefoot deformities as adduction and abduction. Inversion and eversion are complex deformities involving the whole foot [1].

In adults, the anatomical axis of the foot passes through the centre of the second metatarsal head and the centre of the calcaneal tuberosity. The mechanical axis of the foot passes through the centre of the first metatarsal head and the centre of the calcaneal tuberosity. The weight-bearing platform of the foot is represented by a triangle drawn between the centre of the first metatarsal head, the centre of the fifth metatarsal head and the centre of the calcaneal tuberosity [2] (Fig. 1).



FIGURE 1 The weight-bearing platform of the foot. The weight-bearing platform of the foot is represented by a triangle drawn between the centre of the calcaneal tuberosity (*A*), the centre of the first metatarsal head (*B*) and the centre of the fifth metatarsal head (*C*)

Ankle

The ankle is a complex joint consisting of the distal tibia, distal fibula and talus, whose relationship and normal values have not been specifically validated in children.

In the anteroposterior (AP) and lateral (LAT) projections of the ankle joint, the inclination of the distal tibial articular surface can be assessed by the lateral and anterior distal tibial angles. The lateral inclination of the lateral joint surface of the distal tibia is called the “ankle valgus” (as opposed to the “ankle varus”).

To assess the relationship between the distal fibula, distal tibia and talus, we can refer to some measurements traditionally used in the assessment of ankle syndesmosis injuries, such as total clear space, tibiofibular overlap, medial clear space and talocrural angle. They are performed on a mortise view, an AP projection of the ankle with the foot rotated inward 10–20° [2]. In the mortise view, the base of the fifth metatarsal bone projects vertically under the centre of the talar dome.

Lateral Distal Tibial Angle

(Fig. 2)

- Lines: distal tibial articular surface/long axis of the tibia.
- In the AP view: in young children, there is usually a slight valgus angle that approaches 90° by age 10; $89^\circ \pm 3^\circ$ in adulthood [1, 3].



FIGURE 2 Lateral distal tibial angle. The angle between the lines drawn with respect to the distal tibial articular surface and the long axis of the tibia, in the AP view

Anterior Distal Tibial Angle

(Fig. 3)

- Lines: distal tibial articular surface/long axis of the tibia.
- In the lateral view: $79.8 \pm 1.60^\circ$ in adulthood [4].

FIGURE 3 Anterior distal tibial angle. The angle between the lines drawn with respect to the distal tibial articular surface and the long axis of the tibia, in the lateral view



Total Clear Space

(Fig. 4)



FIGURE 4 Measurement of total clear space (TCS), tibiofibular overlap (TFO) and medial clear space (MCS), in the mortise view. TCS (A, yellow line): distance between the medial margin of the fibular groove (posterior border of the tibia) and the medial border of the fibula, measured 10 mm (dotted line) above the tibial plafond. TFO (B, black line): distance between the lateral border of the distal tibia and the medial border of the fibula, measured 10 mm (dotted line) above the tibial plafond. MCS (C, white line): distance between the lateral border of the medial malleolus and the medial border of the talus, measured 5 mm (dotted line) below the tibial plafond

- Distance between the medial margin of the fibular groove (posterior border of the tibia) and the medial border of the fibula, measured 10 mm above the tibial plafond.
- On the mortise view: <4 mm.
- Excessive distance suggests syndesmotic injury.

Tibiofibular Overlap

- Distance between the lateral border of the distal tibia and the medial border of the fibula, measured 10 mm above the tibial plafond.
- On the mortise view: >1 mm.
- Reduced tibiofibular overlap on the mortise view suggests syndesmotic injury.

Medial Clear Space

- Distance between the lateral border of the medial malleolus and the medial border of the talus, measured 5 mm below the tibial plafond.
- On the mortise view: ≤ 5 mm.
- Widening of the distance suggests syndesmotic injury.

Talocrural Angle

(Fig. 5)

- Formed by a line perpendicular to the distal tibial articular surface and a line connecting the distal ends of the malleoli.
- On the mortise view: $83^\circ \pm 4^\circ$.
- Increased angle ($>87^\circ$) suggests syndesmotic injury.

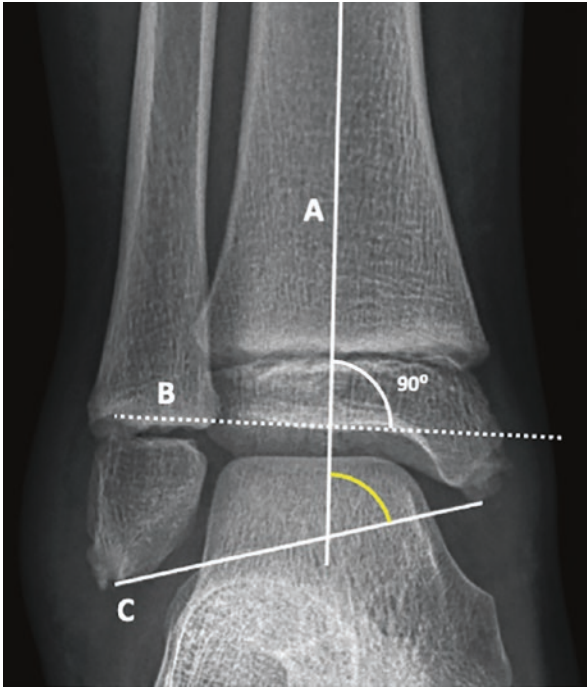


FIGURE 5 Talocrural angle. The angle formed by a line (A) perpendicular to the distal tibial articular surface (B) and a line (C) connecting the distal ends of the malleoli, in the mortise view

Foot

Most qualitative and quantitative assessments are based on the dorsoplantar (AP) and lateral (LAT) radiographic views, which must be obtained either in weight-bearing or simulated

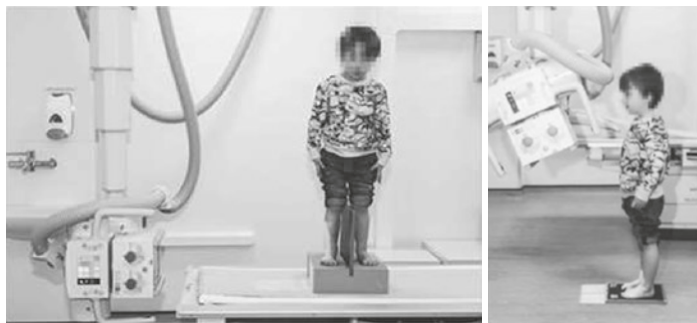


FIGURE 6 Position for lateral and AP standing radiograph. (Courtesy of Cassar-Pullicino and Davies [5])

weight-bearing (dorsiflexion stress), which allows proper configuration of the bony skeleton in its physiologic function to transmit load, adapt to surface conditions or act as a lever for progression.

The AP view is obtained with the patient standing (or in dorsiflexion stress), with the tibia perpendicular to the cassette and the central ray inclined 15° from the vertical line. The lateral view is taken with the patient standing (or in dorsiflexion stress) with the tibia parallel to the cassette (Fig. 6).

In some cases (e.g. diagnosis of foot deformities in infants, including congenital vertical talus and equinovarus), a lateral view in maximum dorsiflexion can be performed. Evaluation of the Bohler and Gissane angles requires superimposition of both malleoli, with the central beam overlying the malleoli [5].

To evaluate the coronal hindfoot alignment with the Meary and Djian methods, a Meary-Tomeno view is needed (Fig. 7): this is an anterior view of the ankle in slight medial rotation, with the heel elevated by a radiolucent wedge (2–3 cm) and the hindfoot enclosed (lead wires on the coronal plane around the malleoli) to reveal plantar support. The tibiotalar line must be horizontal. It allows a quantification of hindfoot valgus or varus and to assess non-operative corrective intervention (adding a heel pad to reduce the deformity) [6, 7]. The Saltzman and El-Khoury distance and the Lamm



FIGURE 7 Maery-Tomeno view. The Maery-Tomeno view is an anterior view of the ankle in slight medial rotation, with the heel elevated by a radiolucent wedge and the hindfoot enclosed (lead wires perpendicular to the malleoli) to reveal plantar support. The tibiotalar line must be horizontal. Note the normal inclination (around 23°) of the subtalar joint line to the horizontal (white arrows)

angle can complete the evaluation of hindfoot deformity in a coronal view, as described below in the specific sections [8, 9]. One must be aware that the measurements taken in these views are not validated in children.

Hindfoot

Since the talus is the only bone with no direct muscular connection to the foot, its hindfoot alignment is assessed by analysing the relationship between the talus and calcaneus through the midtalar line and the midcalcaneal line.

The navicular should typically align with the talus. Malalignment of the hindfoot often results in talonavicular subluxation.

The position of the usually dorsally flexed calcaneus is described in relation to the tibia and talus by the tibiocalcaneal angle and the talocalcaneal angle, respectively. The position of the calcaneus in relation to the ground is described by both the talo-horizontal angle and the calcaneal-horizontal angle.

Hindfoot deformity in the coronal plane can be evaluated with the Meary and Djian methods [6, 7], the Saltzman and El-Khoury distance and the Lamm angle [8, 9]. These measurements, however, are not specifically validated in children.

In addition, two angles related to the morphology of the calcaneus can be used in the evaluation of calcaneal fractures: the Bohler angle and the Gissane angle.

Midtalar Line

(Fig. 8)

- In AP and lateral views, it is drawn along the central axis of the bone.
- In the AP view, it runs drawn between the midpoints of two lines through opposite points on the talus margins at the widest and narrowest points of the talus head and neck.
- In the AP view, in very young children, it runs parallel to the medial cortex of the ossification centre.
- In the AP view, in normal individuals, it passes through or slightly medial to the base of the first metatarsal.



FIGURE 8 Midtalar line. **(a)** In this lateral view, the midtalar line (*A*) has been drawn as a perpendicular line through the midpoint (solid dot) of a line (dotted line) through the superior and inferior borders (circles) of the talonavicular articular surface. **(b)** In this AP view, the midtalar line (*A*) has been drawn between the midpoints (solid dots) of two lines (dotted lines) through opposite points on the talus margins at the widest and narrowest points (circles) of the talus head and neck. It passes slightly medial to the base of the first metatarsal bone

- In the hindfoot valgus, the midtalar line runs medial to the base of the first metatarsal (e.g. pes planus); in the hindfoot varus, the line runs lateral to the base of the first metatarsal (e.g. congenital equinovarus) [1].
- In the lateral view, it is drawn as a perpendicular line through the midpoint of a line through the superior and inferior borders of the talonavicular articular surface.

Midcalcaneal Line

(Fig. 9)

- In the AP and lateral views, it is drawn along the central axis of the bone.
- In the AP view, it may be drawn between the anteromedial corner of the calcaneus and the midpoint of the posterior margin of the calcaneus, or as a tangent to the lateral calcaneal cortex.
- In the AP view, in very young children, it runs parallel to the lateral cortex of the ossification centre.



FIGURE 9 Midcalcaneal line. (a) In this lateral view, the midcalcaneal line (A) has been drawn between the anterior extension of the calcaneal tuberosity on the plantar side and the anteroinferior corner of the calcaneus that articulates with the cuboid. (b) In this AP view, the midcalcaneal line (A) has been drawn as a tangent to the lateral calcaneal cortex. It passes through the base of the fourth metatarsal

- In the AP view, in normal individuals, it passes through the base of the fourth metatarsal.
- In the lateral view, it is drawn between the anterior extension of the calcaneal tuberosity on the plantar side and the anteroinferior corner of the calcaneus that articulates with the cuboid.

Lateral Tibiocalcaneal Angle

(Fig. 10, Tables 1 and 2)

- Lines: distal tibial shaft/midcalcaneal line.
- In the lateral view: 78° (59° ; 96°) in the newborn and 68° (56° ; 80°) by age 4 years [10].
- In the lateral/maximum dorsiflexion view: 41° (25° ; 60°) in the newborn and 52° (30° ; 74°) by age 4 years [10].
- An excessive tibiocalcaneal angle is observed in equinus deformity (congenital equinovarus, rocker bottom deformity).
- A reduced tibiocalcaneal angle is observed in calcaneus deformity (calcaneocavus).



FIGURE 10 Lateral Tibiocalcaneal angle. The angle between the distal tibial shaft (A) and the midcalcaneal line (B), in the lateral view

TABLE 1 Changes in lateral weight-bearing tibiocalcaneal angle during growth (adapted from Vanderwilde et al. [10])

Age (years)	Mean (°)	-2SD (°)	+2SD (°)
0	77.9	59.2	96.1
1	74.3	57.9	91.2
2	71.7	56.4	87.3
3	69.5	56.3	83.5
4	67.7	56.3	80.1
5	66.8	57.1	77.8
6	66.6	58.1	76.5
7	67.1	59.7	75.1
8	67.9	61.7	74.1
9	69.3	64.7	74.1

SD standard deviation

TABLE 2 Changes in lateral maximum dorsiflexion tibiocalcaneal angle during growth (adapted from Vanderwilde et al. [10])

Age (years)	Mean (°)	-2SD (°)	+2SD (°)
0	41.3	24.8	59.8
1	45.4	25.7	65.9
2	48.0	27.6	69.2
3	49.7	28.9	72.3
4	51.7	30.3	73.6
5	52.6	32.6	73.4
6	52.8	34.6	71.9
7	52.2	36.2	70.4

SD standard deviation

Talocalcaneal Angle

(Fig. 11, Tables 3, 4, and 5)

- Lines: midcalcaneal/midtalal lines.
- In the AP view: 42° (27° – 56°) in the newborn and 34° (24° – 44°) by age 4 years [10].
- In the lateral view: 39° (23° ; 56°) in the newborn, 45° (33° – 57°) by age 4 years and then decreasing [10].
- In the lateral/maximum dorsiflexion view: 46° (35° – 56°) in the newborn and 43 (33° – 53°) by age 4 years [10].
- An excessive talocalcaneal angle (usually $>45^\circ$ [1]) is observed in valgus deformity (pes planus, skew foot).

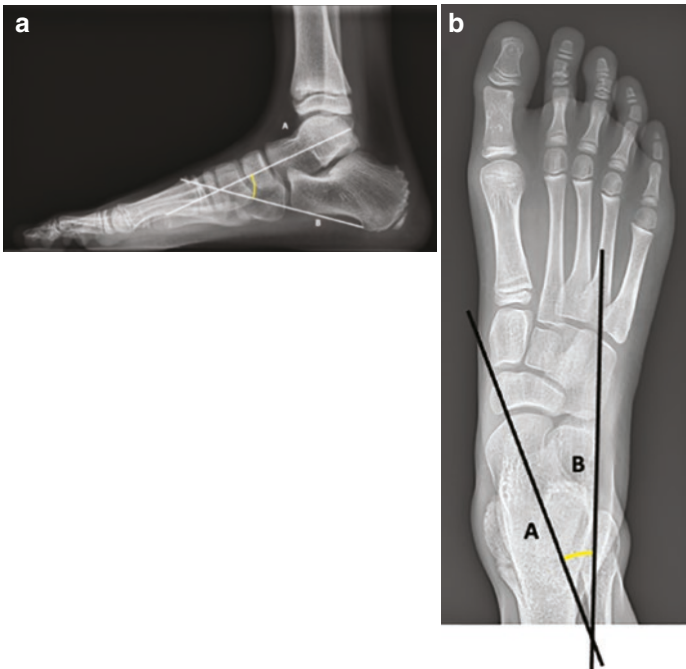


FIGURE 11 Talocalcaneal angle. (a) The angle between the midtalal line (A) and the midcalcaneal line (B), in the lateral view. (b) The angle between the midtalal line (A) and the midcalcaneal line (B), in the AP view

TABLE 3 Changes in AP weight-bearing talocalcaneal angle during growth (adapted from Vanderwilde et al. [10])

Age (years)	Mean (°)	-2SD (°)	+2SD (°)
0	41.9	27.4	56.4
1	40.1	27.1	52.9
2	37.7	26.0	49.9
3	35.7	25.4	46.8
4	33.6	24.0	44.2
5	31.7	22.2	41.3
6	29.5	19.5	39.6
7	27.1	17.5	37.0
8	24.7	14.8	35.3
9	21.6	11.2	33.4

SD standard deviation

TABLE 4 Changes in lateral weight-bearing talocalcaneal angle during growth (adapted from Vanderwilde et al. [10])

Age (years)	Mean (°)	-2SD (°)	+2SD (°)
0	38.8	23.0	55.5
1	41.2	27.1	55.5
2	43.3	29.6	56.4
3	44.4	31.6	56.9
4	45.0	32.9	56.7
5	45.3	33.5	56.1
6	44.4	33.5	55.6
7	43.7	32.5	54.8
8	42.1	30.5	53.6
9	39.7	28.4	51.4

SD standard deviation

TABLE 5 Changes in lateral maximum dorsiflexion talocalcaneal angle during growth (adapted from Vanderwilde et al. [10])

Age (years)	Mean (°)	-2SD (°)	+2SD (°)
0	45.7	34.5	56.2
1	44.8	33.8	55.0
2	43.7	33.5	54.1
3	43.0	32.9	53.4
4	42.5	32.6	52.7
5	42.1	32.1	52.0
6	41.3	31.7	51.8
7	41.4	31.0	51.9
8	40.8	30.7	51.4
9	40.3	30.4	51.4

SD standard deviation

- A reduced talocalcaneal angle (usually $<20^\circ$ [11]) is observed in varus deformity (congenital equinovarus, cavovarus).
- The talocalcaneal angle on lateral/maximum dorsiflexion view is a technical measure of outcome following correction of congenital equinovarus in infants who have not started to walk [5].

Talo-Horizontal Angle

(Fig. 12, Table 6)

- Lines: midtalar line/ground line.
- In the lateral view: 35° (14° – 56°) in the newborn and 30° (20° – 39°) by age 4 years [10].
- This measure is not used in clinical routine [5].
- An excessive talo-horizontal angle is observed in pes planus (planovalgus [2], vertical talus [5]).
- A reduced talo-horizontal angle is observed in pes cavus [2] and congenital equinovarus [5].



FIGURE 12 Talo-horizontal angle. The angle between the midtalar line (A) and the ground line (B), in the lateral view

TABLE 6 Changes in lateral weight-bearing talo-horizontal angle during growth (adapted from Vanderwilde et al. [10])

Age (years)	Mean (°)	-2SD (°)	+2SD (°)
0	35.1	13.5	55.7
1	33.0	15.7	49.9
2	32.1	17.9	46.1
3	31.1	19.4	42.6
4	30.0	19.7	39.1
5	28.9	19.9	37.6
6	28.1	19.4	36.4
7	26.9	17.2	35.6
8	26.1	15.7	35.6
9	25.3	13.9	36.0

SD standard deviation



FIGURE 13 Calcaneal-horizonal angle. The angle between the midcalcaneal line (A) and the ground line (B), in the lateral view

Calcaneal-Horizonal Angle

(Fig. 13)

- Lines: midcalcaneal/ground line.
- In the lateral view: between 20° and 30° [5].
- An excessive angle (greater than 30°) is observed in congenital equinovarus, with cavus deformity, and calcaneocavus [5].
- A reduced angle (smaller than 20°) is observed in pes planovalgus [5].

Meary Method

(Fig. 14)

- In the Meary-Tomeno view.
- This method examines the projection of the tibial axis in relation to the heel contact area (divided in three portions). The tibial axis is defined by the vertical line passing through the centre of the talar dome or by the perpendicular to the tangent to the talar dome passing through the centre of the dome [6, 7].



FIGURE 14 Meary method. This method examines the projection of the tibial axis (A) in relation to the heel contact area (B, divided in three portions). The tibial axis is defined in this picture by the perpendicular (A) to the tangent to the talar dome (D) passing through the centre of the dome (black dot, C). In normal individuals, the tibial axis intersects the heel support zone at the junction of the medial 1/3 and central 1/3. In this picture, the tibial axis intersects the heel support zone in the medial 1/3 portion (valgus of the hind-foot)

- Normal: the tibial axis intersects the heel support zone at the junction of the medial 1/3 and central 1/3; therefore, there is physiological valgus of the hindfoot.
- Valgus of the hindfoot: the tibial axis intersects the heel support zone in the medial 1/3 portion.
- Varus of the hindfoot: the tibial axis approaches the middle of the support area.

Djian Method

(Fig. 15)

- In the Meary-Tomeno view.
- The angle between the vertical and the straight line connecting the centre of the malalignment zone (subtalar joint or, more rarely, the dome of the talus) with the centre of the heel support zone is measured [7].
- Normal: physiological valgus of 3–5°.
- Valgus: Djian angle is increased.
- Varus: the Djian angle is decreased.

Saltzman and El-Khoury Distance

- The hindfoot alignment view (Fig. 16): subjects stand on a radiolucent platform with equal weight on both feet. Two positions are possible: the straight position and the natural position. In the straight position, subjects stand on the platform facing the film with the medial edge of the feet parallel and the knees extended. In the natural position, subjects stand on the platform with the imaged side in the same orientation as in the straight position and with the non-imaged side in a natural external rotation. The X-ray cassette is at an angle of 20° to the vertical. A 3×2×60 mm lead strip is placed tangential to the most posterior aspect of the heel and is oriented perpendicular to the long axis



FIGURE 15 Djian method. The angle between the vertical (*A*) and the straight line (*B*) connecting the centre (black dot) of the malalignment zone (subtalar joint in this picture, line *C*) with the centre (white dot) of the heel support zone (*D*) is measured

of the foot. The X-ray tube is angled 20° from horizontal so that it is perpendicular to the film plane. The beam is centred at the level of the ankle; the field of view extends from

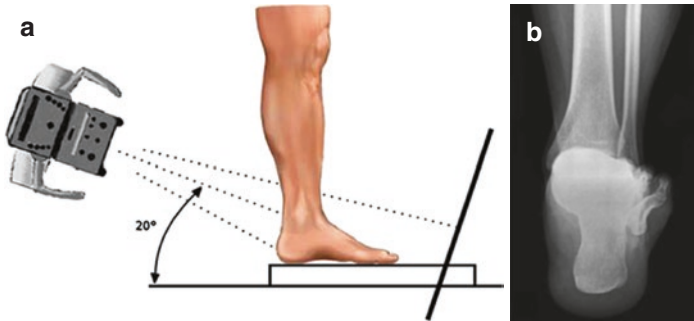


FIGURE 16 The hindfoot alignment view. (Courtesy of Reilingh et al. [12]). (a) Subjects stand on a radiolucent platform in the straight position or in the natural position. The X-ray cassette is at an angle of 20° to the vertical. A lead strip is placed tangential to the most posterior aspect of the heel (not pictured). The X-ray tube is angled 20° from horizontal so that it is perpendicular to the film plane. The beam is centred at the level of the ankle [8]. (b) Radiograph showing the hindfoot alignment view

the middle of the tibia to below the calcaneus. The distance between the source and the film is 1.016 m [8].

- The tibio-calcaneal alignment in the coronal plane (or apparent moment arm) is defined by measuring the horizontal distance on the marker line (i.e. the plane of the floor in the coronal plane) between two lines defined as follows [8]:
 - The first line is a line corresponding to the weight-bearing axis of the leg represented by the mid-longitudinal axis of the tibia (defined by bisecting the tibia 10 and 15 cm above the medial tibial plafond).
 - The second line is the perpendicular to the lead marker line passing through the lowest aspect of the calcaneus (the point under the calcaneus closest to the lead marker line).

- Apparent moment arm values are given:
 - A positive sign when the weight-bearing axis of the leg falls medial to the lowermost point of the calcaneus (valgus calcaneus).
 - A negative sign when the weight-bearing axis of the leg falls lateral to the lowermost point of the calcaneus (varus calcaneus).
- Normal values in straight position: -3.2 ± 7.2 mm [8].
- Normal values in natural position: -1.6 ± 7.2 mm [8].
- It is not validated in children.

Lamm Angle

- The long axial view (Fig. 17): the long leg calcaneal axial view captures the distal third of the tibia, the subtalar joint and the calcaneus. In this view, the patient is in the ski-

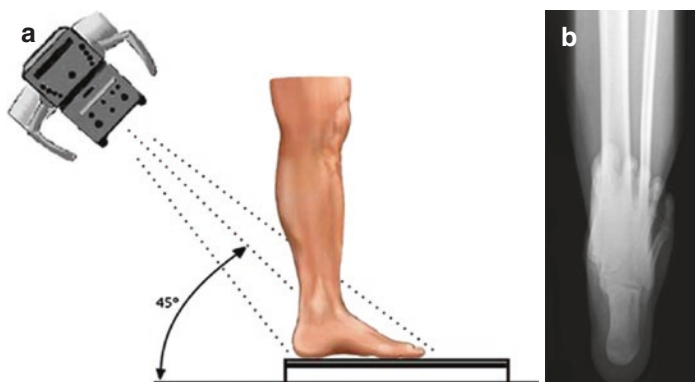


FIGURE 17 The long axial view. (Courtesy of Reilingh et al. [12]). (a) According to Lamm et al. [9], the patient is in the ski-jumping position (not pictured). The affected limb is in the centre of the film. The heel is closest to the edge of the film. The central ray is centred on the subtalar joint. The head of the tube is behind the affected limb and is inclined at a 45° angle to the vertical. (b) Radiograph showing the long axial view

jumping position: the affected ankle is in maximum dorsiflexion and the knee is extended. The affected limb is in the centre of the film and the unaffected limb is in front of the film. The heel is closest to the edge of the film. The central ray is centred on the subtalar joint. The head of the tube is behind the affected limb, 1.016 m from the heel, and is inclined at a 45° angle to the vertical [9].

- The angle between the mid-diaphyseal line of the tibia and the calcaneal bisection line is evaluated. The calcaneal bisection line (i.e. the frontal plane axis of the posterior heel) is obtained from the bisector of the radiographic silhouette of the calcaneus [9].
- Normal value: 2.1° of varus [9].
- It is not validated in children.

Bohler Angle

(Fig. 18, Table 7)

- Lines: from the posterior corner of the calcaneal apophysis to the proximal edge of the posterior facet/from the proximal edge of the posterior facet to the superior anterior aspect of the calcaneus at the calcaneocuboid joint [13].
- In the lateral view, with superimposition of both malleoli: 34° under the age of 5, 40° between 5 and 8 years of age and 33° between 13 and 16 years of age [14].
- It is used to assess the calcaneus deformity due to fracture; in particular, if the fracture involves the anterior process of the calcaneus, the angle decreases [2, 5].



FIGURE 18 Bohler's angle. The angle between the lines drawn from the posterior corner of the calcaneal apophysis (*A*) to the proximal edge of the posterior facet (*B*) and from the proximal edge of the posterior facet (*B*) to the supero-anterior aspect of the calcaneus at the calcaneocuboid joint (*C*)

Gissane Angle

(Fig. 19, Table 7)

- Lines: posterior facet/middle facet.
- In the lateral view, with superimposition of both malleoli: 116° under the age of 5, 111° between 5 and 8 years of age and 110° between 13 and 16 years of age [14].
- It is used to assess the deformity of the calcaneus due to fracture [2, 5].



FIGURE 19 Gissane's angle. The angle between the posterior facet (A) and the middle facet (B) of the calcaneus

TABLE 7 Changes in Bohler and Gissane angles during growth (adapted from Pombo et al. [14])

Age (years)	Bohler angle (mean \pm SD; $^{\circ}$)	Gissane angle (mean \pm SD; $^{\circ}$)
0–4	33.6 \pm 5.5	115.8 \pm 7.3
5–8	39.7 \pm 5.7	111.1 \pm 7.5
9–12	35.1 \pm 5.5	109.8 \pm 7.2
13–16	33.0 \pm 5.0	109.8 \pm 7.1
0–16	35.4 \pm 5.9	110.5 \pm 7.4
≥ 18	31.7 \pm 5.2	112.8 \pm 7.4

SD standard deviation

Midfoot

Changes in hindfoot alignment are usually reflected in altered relationships between the hindfoot and midfoot. The navicular plays a pivotal role, yet it is the last bone to ossify. If it is not yet ossified, assessment of alignment depends on the metatarsal bases; the lateral cuneiform, which begins to ossify between the neonatal period and 19 months of age, may also help to indicate midfoot and hindfoot deformity.

In congenital clubfoot, ultrasonography is increasingly advocated for assessing deformity at birth and tracking treatment outcomes because it can visualise the cartilaginous attachments of the growing feet [15, 16].

To assess tarsal alignment, the tarsal joint surface angles can be measured on a lateral view; however, these measurements have not been validated in children.

The plantar arch is also best assessed in the lateral view by measuring the alignment of the hindfoot and metatarsals: the posterior portion of the arch is represented by the dorsally flexed calcaneus; the plantar angulation of the distal metatarsal bones forms the anterior portion of the arch. Several angles can be measured, including the Meary angle, the Djian-Annonier angle, the lateral calcaneus-fifth-metatarsal angle and the lateral calcaneus-first-metatarsal or Hibbs angle.

Ultrasound Measurements

(Fig. 20, Table 8)

- On medial view: in neutral position of the foot; by positioning the transducer at the medial border of the foot, in a slightly oblique position; a plane showing the medial malleolus, the lateral malleolus and the navicular is chosen.
 - The medial malleolus-navicular distance: the shortest distance between the medial malleolus and the medial part of the navicular:

Normal value at birth: 8.5 ± 1.1 mm [17].

Decreased distance in congenital clubfoot (4.6 ± 1.7 mm) [15].

- The soft tissue thickness: the perpendicular distance from the skin surface to the medial border of the cartilaginous talus at the level of the midpoint of the ossification centre:

Normal value at birth: 4.7 ± 0.7 mm [17].

Increased thickness in congenital clubfoot (11.6 ± 2.0 mm) [15].

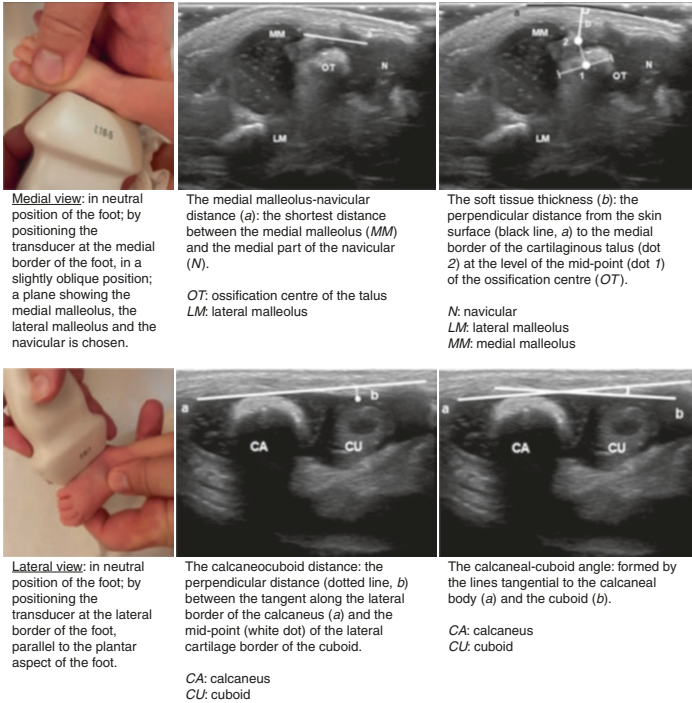


FIGURE 20 Ultrasound measurements

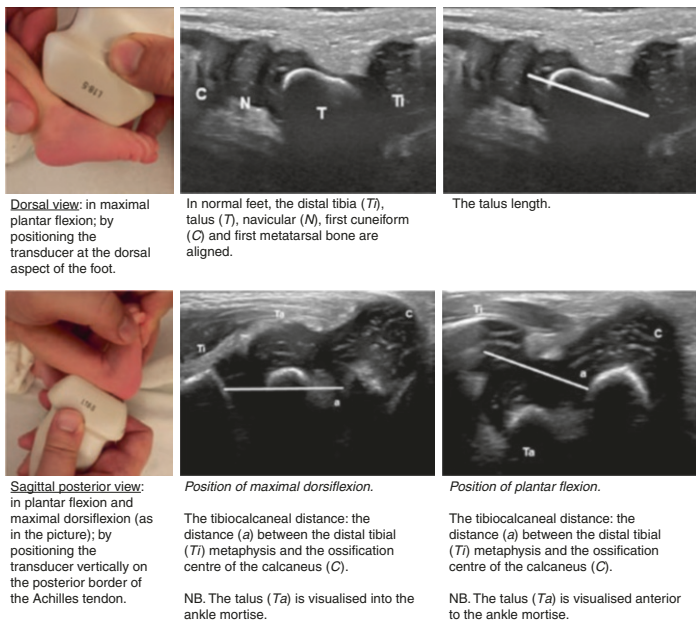


FIGURE 20 (continued)

- On lateral view; in neutral position of the foot; by positioning the transducer at the lateral border of the foot, parallel to the plantar aspect of the foot:
 - The calcaneocuboid distance: the perpendicular distance between the tangent along the lateral border of the calcaneus and the midpoint of the lateral cartilage border of the cuboid:

Normal value at birth: 1.16 ± 1.1 mm [17].

Increased distance in congenital clubfoot (2.5 ± 1.3 mm) [15].
 - The calcaneal-cuboid angle: formed by the lines tangential to the calcaneal body and the cuboid:

Normal value: $<12^\circ$ [16]. (Newborn: <45 days).

Increased angle in congenital clubfoot: mean 20° (range $16\text{--}32^\circ$) [16]. (Newborn: <45 days).

TABLE 8 Changes in ultrasound measurements of the infant's foot during growth (adapted from Aurell et al. [15])

Age (months)	Medial malleolus-				Length of talus (mean \pm SD; mm)
	navicular distance (mean \pm SD; mm)	Calcaneocuboid distance (mean \pm SD; mm)	Soft tissue thickness (mean \pm SD; mm)		
0	8.5 \pm 1.1	1.16 \pm 1.1	4.7 \pm 0.7		177 \pm 1.1
4	9.7 \pm 1.3	2.1 \pm 1.2	5.5 \pm 1.0		21.0 \pm 1.3
7	10.8 \pm 1.3	3.0 \pm 1.1	6.2 \pm 1.3		23.1 \pm 1.6
12	12.3 \pm 1.3	2.8 \pm 1.3	7.6 \pm 1.0		—

SD standard deviation

On dorsal view: in maximal plantar flexion; by positioning the transducer at the dorsal aspect of the foot. In normal feet, the talus, navicular, first cuneiform and first metatarsal bone are aligned. In clubfoot, the navicular is medially displaced [16].

- The talus length:

Normal value at birth: 177 ± 1.1 mm [17].

Decreased length in congenital clubfoot (14.5 ± 1.2 mm) [15].

- On sagittal posterior projection: in plantar flexion and maximal dorsiflexion; by positioning the transducer vertically on the posterior border of the Achilles tendon:

- The tibiocalcaneal distance: the distance between the distal tibial metaphysis and the calcaneal apophysis:

Normal values: mean 10 mm (range 8.5–12.5 mm) in plantar flexion; mean 20 mm (range 15–23 mm) in maximal dorsiflexion [16]. (Newborn: <45 days old).

Decreased distance in maximal dorsiflexion in congenital clubfoot: mean 10.5 mm (range 9.5–11.5 mm) [16] (Newborn: <45 days old).

Lateral Tarsal Joint Surface Angles

(Fig. 21)

- Lines: parallel to the floor/lines drawn through the tarsal articular surfaces.
- In the lateral view, the articular surfaces of the talonavicular, the navicular-cuneiform and the first tarsometatarsal joints should show an approximately parallel alignment.
- The following normal ranges have been reported:
 - Talonavicular joint: $54\text{--}74^\circ$.
 - Navicular-cuneiform joint: $51\text{--}68^\circ$.
 - First tarsometatarsal joint: $55\text{--}72^\circ$.
- It is not validated in children.



FIGURE 21 Lateral Tarsal joint surface angles. The angles between the parallel to the ground floor (A) and the lines drawn through the tarsal articular surfaces: (B) line through talonavicular joint, (C) line through naviculocuneiform joint, (D) line through first tarsometatarsal joint

Lateral Talar-First Metatarsal or Meary Angle

(Fig. 22, Table 9)

- Lines: midtalar line/first metatarsal shaft (the first metatarsal is easily distinguished as the shortest widest metatarsal).
- In the lateral view: near 0° ; 19° (-2° ; 40°) in the newborn and 8° (-5° ; 21°) by age 4 years.
- Positive angles (usually $>4^\circ$ [2]) denote pes planus.
- Negative angles (usually $<-4^\circ$ [2]) denote pes cavus.

Djian-Annonier Angle

(Fig. 23)

- The angle between the most inferior point of the calcaneus, the most inferior point of the talonavicular joint and the most inferior point of the medial sesamoid (not visible in young children).



FIGURE 22 Talar-first metatarsal or Meary angle. The angle between the midtalar line (A) and the first metatarsal shaft (B). Positive angles denote a pes planus. Negative angles denote a pes cavus

TABLE 9 Changes in lateral weight-bearing talar / first metatarsal angle during growth (adapted from Vanderwilde et al. [10])

Age (years)	Mean (°)	-2SD (°)	+2SD (°)
0	18.5	-2.4	40.2
1	15.7	-3.6	34.2
2	12.4	-3.7	29.0
3	10.1	-4.9	24.3
4	8.3	-5.4	21.1
5	6.9	-5.7	19.8
6	5.6	-6.3	17.6
7	5.6	-6.6	17.2
8	5.6	-6.4	17.4
9	5.2	-6.9	18.9

Positive angles denote a planovalgus posture
SD standard deviation



FIGURE 23 Djian-Annonier angle. The angle between the most inferior point of the calcaneus (A), the most inferior point of the talonavicular joint (B) and the most inferior point of the medial sesamoid (C)

- In the lateral view, normal values: 120° – 130° [7, 18].
- Angles $>130^{\circ}$ denote a pes planus [7, 18].
- Angles $<120^{\circ}$ denote a pes cavus [7, 18].
- It's not validated in children.

Lateral Calcaneus-Fifth Metatarsal Angle

(Fig. 24)

- Lines: tangent to the inferior border of the calcaneus/fifth metatarsal shaft.
- In the lateral view: between 150° and 175° (apex upward) [2].
- A reduced angle with apex upward is observed in pes cavus [2].
- An excessive angle with apex upward is observed in pes planus [2].
- An excessive angle with apex downward is observed in congenital equinovarus and rocker bottom deformity [2].



FIGURE 24 Lateral Calcaneus-fifth metatarsal angle. The angle between the tangents to the inferior border of the calcaneus (A) and the fifth metatarsal shaft (B)

Lateral Calcaneus-First Metatarsal or Hibbs Angle

(Fig. 25)

- Lines: midcalcaneal/first metatarsal shaft.
- In the lateral view: 150° [1].
- A reduced angle (usually $<140^\circ$ [1]) is observed in pes cavus.

Forefoot

Relative metatarsal lengths can be assessed using various methods such as the metatarsal index, Morton's method, Hardy and Clapham's method and metatarsal depth angle; however, these methods have not been validated in children.

Forefoot adduction and abduction describe the metatarsal position solely in the plane of the foot, without inversion or eversion of the plantar surface. In an AP projection, the metatarsals essentially move as a unit toward (adduction) or away from (abduction) the midline, pivoting at their bases; in a



FIGURE 25 Lateral Calcaneus-first metatarsal or Hibbs angle. The angle between the midcalcaneal line (A) and the first metatarsal shaft (B)

lateral projection, the normal superimposition of the central metatarsals is maintained (unless there is an associated inversion or eversion).

Inversion and eversion are complex deformities of the entire foot.

Inversion combines supination, adduction and plantar flexion: in the AP view, metatarsal bases are superimposed and distal metatarsals swing toward the midline; in the lateral view, a ladder-like array may be seen, with the fifth metatarsal more plantar than the first one.

Eversion combines pronation, abduction and dorsiflexion: in the AP view, there is increased separation of the metatarsal bases and the metatarsal shafts are more parallel and less divergent; in the lateral view, a ladder-like array may be seen, with the first metatarsal more plantar than the fifth.

The relationship between metatarsals can be evaluated through the metatarsus adductus angle, the modified metatarsus adductus angle, the angle between the long axes of the calcaneus and the second metatarsal, the AP talar-first metatarsal angle and the AP calcaneal-fifth metatarsal angle.

Also, the presence of hallux valgus has to be evaluated.

Metatarsal Index

(Fig. 26)

- Line: uniform arc across the distal ends of the second through the fifth metatarsal.

FIGURE 26 Metatarsal index. The relationship between the head of the first metatarsal (dotted line) and a uniform arc across the distal ends of the second through the fifth metatarsal (continuous line). In this picture, we observe a minus index: the first metatarsal head is proximal to the arc.



- In the AP view, observing the relationship between the head of the first metatarsal and the line, we can distinguish:
 - Plus index: the first metatarsal head is distal to the arc.
 - Plus-minus index: the distal end of the first metatarsal head touches the arc.
 - Minus index: the first metatarsal head is proximal to the arc.
- A minus index indicates a predisposition to hallux valgus and metatarsalgia [2].
- It is not validated in children.

Morton's Method

(Fig. 27)

- Line: perpendicular to the longitudinal axis of the second metatarsal, through the head of the second metatarsal.
- On AP view, observing the relationship between the head of the first metatarsal and the line, we can distinguish:
 - Plus rating: horizontal line extends proximal (> 2 mm) to first metatarsal head (long first metatarsal).
 - Minus rating: horizontal line extends distal (>2 mm) to first metatarsal head (short first metatarsal) [19].
- A valgus or varus deformity of the first ray can distort the measurements.
- It is not validated in children.

Hardy and Clapham's Method

(Fig. 28)

- Lines: the axes of the first and second metatarsals are drawn; a transverse tarsal line is drawn to touch the posterior articular surface of the cuboid and the posterior aspect of the tuberosity of the navicular. At the point of intersection of this line with the axis of the second meta-

FIGURE 27 Morton's method. Based on the relationship between the head of the first metatarsal (dotted line) and a reference line (A), perpendicular to the longitudinal axis of the second metatarsal (B), through the head of the second metatarsal. We can distinguish: Plus rating: horizontal line extends proximal to first metatarsal head (long first metatarsal); Minus rating: horizontal line extends distal to first metatarsal head (short first metatarsal)



tarsal (point Z), the point of a pair of dividers is placed; arcs are then drawn to touch the articular surfaces of the heads of the first and second metatarsals.

- In the AP view, the radial distance (in mm) between the arcs is taken as the measure of relative metatarsal protrusion: a positive sign indicates that the first is greater than

FIGURE 28 Hardy and Clapham's method. The axes of the first (*A*) and second (*B*) metatarsals are drawn; a transverse tarsal line (*C*) is drawn to touch the posterior articular surface of the cuboid and the posterior aspect of the tuberosity of the navicular (white dot). At the point of intersection of this line with the axis of the second metatarsal (black dot, *z*), the center of rotation is placed; arcs are then drawn to touch the articular surfaces of the heads of the first (*D*, dotted black curved line) and second (*E*, bold black curved line) metatarsals. The radial distance (*F*) between the arcs is taken as the measure of relative metatarsal protrusion. In this picture, a negative sign indicates that the second metatarsal is greater than the first



the second; a negative sign indicates that the second is greater than the first.

- In the cases of hallux valgus, the first metatarsal is longer (>2 mm) than in the controls [20].
- It is not validated in children.

Metatarsal Depth Angle

(Fig. 29)

- Lines: tangent to the first and the second metatarsal heads/
tangent to the second and the fifth metatarsal heads.
- In the AP view: 142.5° .

FIGURE 29 Metatarsal depth angle. The angle between the tangent to the first and the second metatarsal heads (*A*) and the tangent to the second and the fifth metatarsal heads (*B*)

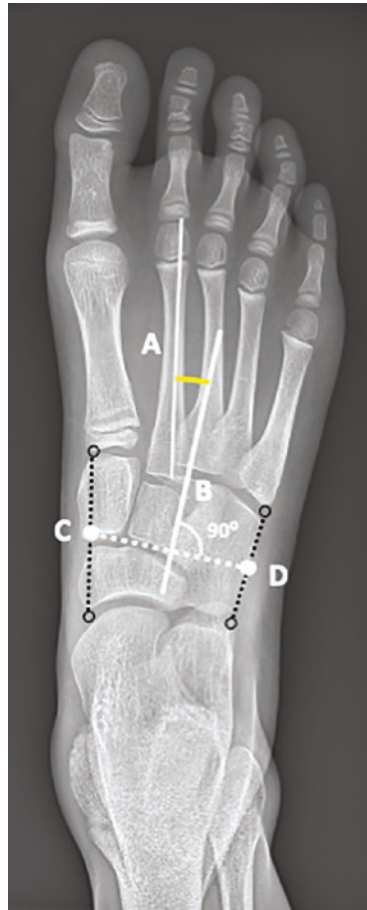


- If the angle is $<135^\circ$, a relative shortening of the first metatarsal can be denoted [2, 21].
- It is not validated in children.

Metatarsus Adductus Angle

(Fig. 30)

FIGURE 30 Metatarsus adductus angle. The angle between the axis of the second metatarsal (*A*) and the perpendicular (*B*) to a line drawn between the midpoint (*C*) between the medial aspect of the first metatarsal-cuneiform joint and the medial aspect of the talonavicular joint; and the midpoint (*D*) between the lateral aspect of the fifth metatarsal-cuboid joint and the lateral aspect of the calcaneocuboid joint



- Lines: axis of the second metatarsal/perpendicular to a line AB, where:
 - A is the midpoint between the medial aspect of the first metatarsal-cuneiform joint and the medial aspect of the talonavicular joint.
 - B is the midpoint between the lateral aspect of the fifth metatarsal-cuboid joint and the lateral aspect of the calcaneocuboid joint.
- Useful only in children whose tarsal bones are mostly ossified.
- In the AP view: between 10° and 20° [2, 5].
- An excessive angle is observed in forefoot adduction [5].

Modified Metatarsus Adductus Angle or Engel's Method

(Fig. 31)

- Lines: axis of the second metatarsal/axis of the medial cuneiform.
- Useful only in children whose tarsal bones are mostly ossified.
- In the AP view: between 13° and 23° [22].
- An excessive angle is observed in forefoot adduction [5].

Angle Between Calcaneus and Second Metatarsal

(Fig. 32)

- Lines: midcalcaneal/second metatarsal axis.
- In the AP view: $\leq 22^\circ$ (mean value 10°) [2].
- It is usually used in newborns and small children when the tarsal bones are not yet fully ossified and the metatarsus adductus angle evaluation can be challenging.
- An excessive angle is observed in forefoot adduction.

FIGURE 31 Modified metatarsus adductus angle or Engel's method. The angle between the axis of the second metatarsal (*A*) and the axis of the medial cuneiform (*B*)



AP Talar-First Metatarsal Angle

(Fig. 33, Table 10)

- Lines: midtalar/first metatarsal axis.
- In the AP view: 21° (9° ; 31°) in the newborn and 10° (-4° ; 24°) by age 4 years [10].

FIGURE 32 Angle between calcaneus and second metatarsal. The angle between the midcalcaneal line (A) and the second metatarsal axis (B)



- The angle usually is between 0° and 20° . A negative angle, with lateral positioning of the midtalar line, can be observed in forefoot adduction and clubfoot [11].
- NB: Simons et al. [11] consider positive angle as pathological and negative as physiological. We used a different definition to be consistent with measurements given by Vanderwilde et al. [10].

FIGURE 33 AP Talar-first metatarsal angle. The angle between the midtalar line (*A*) and the first metatarsal axis (*B*). In the picture a negative angle, with lateral positioning of the midtalar line, can be observed

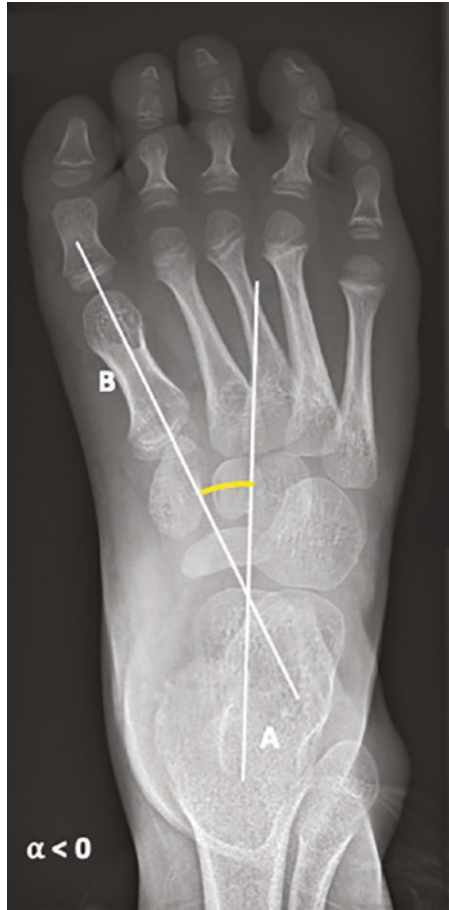


TABLE 10 Changes in AP weight-bearing talar-first metatarsal angle during growth (adapted from Vanderwilde et al. [10])

Age (years)	Mean (°)	-2SD (°)	+2SD (°)
0	20.5	9.1	31.4
1	16.8	5.2	29.5
2	14.6	1.6	27.0
3	12.2	-0.9	25.2
4	10.4	-3.6	23.8
5	8.4	-5.7	22.2
6	6.6	-7.2	20.7
7	5.5	-8.1	19.3
8	3.9	-9.0	18.3
9	3.2	-9.7	17.3

SD standard deviation

AP Calcaneal-Fifth Metatarsal Angle

(Fig. 34, Table 11)

- Lines: midcalcaneal/fifth metatarsal axis.
- In the AP view: 2 (-9° ; 15°) in the newborn, -1 (-10° ; -9°) by age 4 years and then increasing [10].
- Positive angles indicate that the distal projection of the fifth metatarsal is directed more laterally than the axis of the calcaneus.
- Angles can be disturbed in metatarsus adductus [5].

FIGURE 34 AP Calcaneal-fifth metatarsal angle. The angle between the midcalcaneal line (*A*) and the fifth metatarsal axis (*B*). Positive angles indicate that the distal projection of the fifth metatarsal is directed more laterally than the axis of the calcaneus. In the picture, a negative angle indicates that the distal projection of the fifth metatarsal is directed more medially than the axis of the calcaneus



TABLE II Changes in AP weight-bearing calcaneal-fifth metatarsal angle during growth (adapted from Vanderwilde et al. [10])

Age (years)	Mean (°)	-2SD (°)	+2SD (°)
0	2.4	-9.1	14.6
1	0.9	-9.9	11.9
2	-0.4	-10.0	9.9
3	-0.8	-10.2	8.9
4	-1.3	-10.2	8.3
5	-1.2	-10.1	8.5
6	-0.5	-9.9	9.0
7	0.3	-9.1	10.5
8	2.0	-8.8	13.0
9	3.8	-7.4	15.1

SD standard deviation

Hallux Valgus Angle

(Fig. 35)

- Lines: proximal phalanx axis of the first ray/first metatarsal axis.
- In the AP view: $8^\circ \pm 3^\circ$.
- A hallux valgus angle greater than 15° is considered pathological [23].

FIGURE 35 Hallux valgus angle. The angle between the proximal phalanx axis of the first ray (A) and the first metatarsal axis (B)



References

1. Stein-Wexler R, Wootton-Gorges SL, Ozonoff MB. Pediatric orthopedic imaging. Berlin, Heidelberg: Springer-Verlag; 2015. <https://www.springer.com/gp/book/9783642453809>.
2. Waldt S, Woertler K. Measurements and classifications in musculoskeletal radiology. New York: Thieme Verlag; 2014. <https://www.thieme-connect.de/products/ebooks/book/10.1055/b-002-91661>. Accessed 31 Aug 2021.
3. Paley D. Principles of deformity correction. Berlin: Springer Science & Business Media; 2002. p. 860.
4. Paley D, Herzenberg JE, Tetsworth K, McKie J, Bhave A. Deformity planning for frontal and sagittal plane corrective osteotomies. *Orthop Clin North Am*. 1994;25(3):425–65.
5. Cassar-Pullicino VN, Davies AM, editors. Measurements in musculoskeletal radiology. Berlin, Heidelberg: Springer-Verlag; 2020. (Diagnostic Imaging). <https://www.springer.com/gp/book/9783540438533>. Accessed 31 Aug 2021.
6. Neri T, Barthelemy R, Tourné Y. Analyse radiologique de l'alignement de l'arrière-pied: comparaison entre les clichés de Meary, long axial view et hindfoot alignment view. *Revue de Chirurgie Orthopédique et Traumatologique*. 2017;103(8):882–7.
7. Serra-Tosio G. Repères et mesures utiles en imagerie ostéo-articulaire. Issy-les-Moulineaux: Elsevier-Masson; 2011. (Imagerie médicale, pratique).
8. Saltzman CL, El-Khoury GY. The hindfoot alignment view. *Foot Ankle Int*. 1995;16(9):572–6.
9. Lamm BM, Mendicino RW, Catanzariti AR, Hillstrom HJ. Static Rearfoot alignment: a comparison of clinical and radiographic measures. *J Am Podiatr Med Assoc*. 2005;95(1):26–33.
10. Vanderwilde R, Staheli LT, Chew DE, Malagon V. Measurements on radiographs of the foot in normal infants and children. *J Bone Joint Surg Am*. 1988;70(3):407–15.
11. Simons G. Analytical radiography of club feet. *J Bone Joint Surg*. 1977;59-B(4):485–9.
12. Reilingh ML, Beimers L, Tuijthof GJM, et al. Measuring hind-foot alignment radiographically: the long axial view is more reliable than the hindfoot alignment view. *Skeletal Radiol*. 2010;39:1103–8. <https://doi.org/10.1007/s00256-009-0857-9>.
13. Böhler L. Diagnosis, pathology, and treatment of fractures of the OS CALCIS. *J Bone Jt Surg*. 1931;13(1):75–89.

14. Pombo B, Ferreira AC, Costa L. Bohler angle and the crucial angle of Gissane in Paediatric population. *Clin Med Insights Arthritis Musculoskelet Disord*. 2019;12:1179544119835227.
15. Aurell Y, Johansson A, Hansson G, Jonsson K. Ultrasound anatomy in the neonatal clubfoot. *Eur Radiol*. 2002;12(10):2509–17.
16. Gigante C, Talenti E, Turra S. Sonographic assessment of clubfoot. *J Clin Ultrasound*. 2004;32(5):235–42.
17. Aurell Y, Johansson A, Hansson G, Wallander H, Jonsson K. Ultrasound anatomy in the normal neonatal and infant foot: an anatomic introduction to ultrasound assessment of foot deformities. *Eur Radiol*. 2002;12(9):2306–12.
18. Bouysset M. Pathologie ostéo-articulaire du pied et de la cheville: approche médico-chirurgicale. Berlin: Springer Science & Business Media; 2004. p. 602.
19. Karasick D, Wapner KL. Hallux valgus deformity: preoperative radiologic assessment. *AJR Am J Roentgenol*. 1990;155(1):119–23.
20. Hardy RH, Clapham JCR. Observations on hallux valgus; based on a controlled series. *J Bone Joint Surg Br*. 1951;33-B(3):376–91.
21. Gamble FO, Yale I. Clinical foot roentgenology. Malabar, FL: R. E. Krieger Publishing Company; 1975. p. 456.
22. Engel E, Erlick N, Krems I. A simplified metatarsus adductus angle. *J Am Podiatry Assoc*. 1983;73(12):620–8.
23. McCluney JG, Tinley P. Radiographic measurements of patients with juvenile hallux valgus compared with age-matched controls: a cohort investigation. *J Foot Ankle Surg*. 2006;45(3):161–7.